Developmental and Comparative Immunology 87 (2018) 24–35

Contents lists available at ScienceDirect

Developmental and Comparative Immunology

journal homepage: www.elsevier.com/locate/devcompimm

Rag1 and *rag2* gene expressions identify lymphopoietic tissues in juvenile and adult Chinese giant salamander (*Andrias davidianus)*

Nan Jiang[a], Yuding Fan[a], Yong Zhou[a], Wenzhi Liu[a], Jacques Robert[b,*], Lingbing Zeng[a,**]

[a] Division of Fish Disease, Yangtze River Fisheries Research Institute, Chinese Academy of Fishery Sciences, Wuhan, Hubei 430223, China
[b] Department of Microbiology and Immunology, University of Rochester Medical Center, New York 14642, USA

ARTICLE INFO

Keywords:
Andrias davidianus
rag1
rag2
Lymphopoietic tissues

ABSTRACT

Rag1 and *rag2* are two closely linked recombination activating genes required for V(D)J recombination of antigen receptors in immature lymphocytes, whose expression can serve as marker to identify the lymphopoietic tissues. To study the development of lymphopoietic tissues in Chinese giant salamander (*Andrias davidianus*), the Chinese giant salamander *rag1* and *rag2* coding sequences were cloned and determined. High transcript levels of *rag1* and *rag2* were co-detected in the thymus before 14 months of age, whereas levels were lower in spleen, liver and kidney at all stage of development. The spatial expression patterns of *rag1* and *rag2* were studied in combination with *igY* and *tcrβ* gene expression using *in situ* hybridization. Significant transcript signals for *rag1*, *rag2*, *tcrβ* and *igY* were detected not only in the thymus and spleen but also the liver and kidney of juvenile and adult Chinese giant salamanders, which suggests that cells of lymphocyte lineage are present in multiple tissues of the Chinese giant salamander. This implies that lymphopoiesis may take place in these tissues. The tissue morphology of thymus suggested that the branched thymic primordium developed into mature organ with the development of thymocyte from juvenile to adult. These results not only confirm that as expected the thymus and spleen are primordial lymphopoietic tissues but also suggest that the liver and kidney provide site of lymphocyte differentiation in Chinese giant salamander.

1. Introduction

The Chinese giant salamander (*Andrias davidianus*), which belongs to the family *Cryptobranchidae*, is one of the most primitive urodele amphibian species in the world (Zhang et al., 2003). *A. davidianus* is listed in Appendix I of the Convention on International Trade of Endangered Species of Wild Fauna and Flora and in national class II protected species in China (Zhu et al., 2014a). In recent years, outbreaks of infectious disease have become a threat to natural populations and artificial breeding of Chinese giant salamander (Dong et al., 2011; Geng et al., 2011; Chen et al., 2013; Meng et al., 2014; Zhang and Gui, 2015; Gui et al., 2018). For improving disease control, a better characterization of the development of lymphopoietic tissues as well as T and B cell ontogeny in the Chinese giant salamander is of significance both theoretically and practically.

The understanding of immune response of urodele amphibians is relatively poor compared to mammals and anuran amphibians (Tournefier, 1975; Kaufman et al., 1990), although many elements and functions of urodele amphibians are conserved with mammals (Frippiat et al., 2001). The Chinese giant salamander has been shown to possess genes encoding immunoglobulin heavy chains (IgH, IgM, IgY and IgD) genes, T-cell receptor β (TCRβ) and major histocompatibility complex (MHC) molecules (Zhu et al., 2014a, 2014b). In jawed vertebrates, mature T cells and B cells are generated by V(D)J recombination of IG and TCR loci, to produce their specific antigen receptors (Durand et al., 2000). *Rag1* and *rag2* expression correlates with the rearrangement of *ig* and *tcr* transcripts in mice, *Xenopus* and Mexican axolotl (Mombaerts et al., 1992; Shinkai et al., 1992; Fellah et al., 1993; Kerfourn et al., 1996; Hansen and Zapata, 1998). In mammals, mutations in *rag1* and *rag 2* result in loss or reduction of V(D)J recombination, and lack of mature T and B cells (Mombaerts et al., 1992; Shinkai et al., 1992; Ijspeert et al., 2014). As such, *rag1* and *rag 2* serve as useful markers for B cell and T cell differentiation and maturation in the lymphopoietic tissues (Hansen and Zapata, 1998). *Rag* genes and proteins have been conserved during vertebrate evolution from elasmobranchs to mammals (Willett et al., 1997; Durand et al., 2000). Unlike mammals, urodele amphibians and fish lack a hematopoietic bone marrow in which B lymphocytes differentiate (Trede and Zon, 1998; Durand et al., 2000). In *Xenopus*, *rag1* and *rag2* expression has detected in thymus and spleen, which is consistent with their role as major lymphopoietic tissues

* Corresponding author.
** Corresponding author.
E-mail addresses: Jacques_Robert@URMC.Rochester.edu (J. Robert), zlb@yfi.ac.cn (L. Zeng).

https://doi.org/10.1016/j.dci.2018.05.018
Received 26 March 2018; Received in revised form 21 May 2018; Accepted 21 May 2018
Available online 22 May 2018
0145-305X/

(Greenhalgh et al., 1993; Robert et al., 2002). Also, B cell differentiation occurs in the liver of tadpole and adult *Xenopus* (Du Pasquier et al., 2000; Robert and Ohta, 2009), and hepatic B cell lymphopoiesis is associated to the peripheral layer of the liver (Hansen and Zapata, 1998). In zebrafish, common carp and trout, *rag1* is detected mainly in adult thymus and kidney, but not in the spleen, which indicated the thymus and kidney are the major lymphopoietic tissue in teleost (Willett et al., 1997; Huttenhuis et al., 2005). Furthermore, the detection *Rag1* and *igu* transcripts in the pancreas of zebrafish suggest that B cell differentiate in this tissue (Danilova and Steiner, 2002). In *Pleurodeles walti*, the strongest expression of *rag1* is detected in the thymus of juvenile animals, while it is weaker in the spleen and brain of adults (Frippiat et al., 2001). In Mexican axolotl, *rag1* is expressed in thymus until its natural involution after 1 year old, but it becomes undetectable in liver and spleen, 4.5 and 8 months respectively. RAG2 protein was detected in the thymus, spleen and liver of 7-month-old axolotls (Durand et al., 2000). All these studies indicate that, the developments of lymphocytes that rearrange *ig* or *tcr* genes are different among urodele amphibians. Chinese giant salamander *rag1* and *rag2* genes have not been reported yet. Therefore, we determined the *rag1* and *rag2* expression as a way to reveal temporal and spatial patterns of T cell and B cell generation in Chinese giant salamander for the first time.

In this study, we cloned the open reading frame of Chinese giant salamander *rag1* and *rag2* genes and determined the expression patterns by real-time PCR. *In situ* hybridization (ISH) of *rag1* and *rag2* genes were used to determine the anatomical origin and the development of lymphocytes from juvenile to adult Chinese giant salamander. Meanwhile, ISH of *igY* (KJ686320) and *tcrβ* (KJ686333.1) genes were used to identify the developing B cell and T cell. Moreover, we utilized histological analysis in combination with ISH to identify T and B cell lymphopoietic tissues in Chinese giant salamander from juvenile to adult.

2. Materials and methods

2.1. Animals and sampling

All the animal handling and experimental procedures were approved by the Animal Care and Use Committee of the Yangtze River Fisheries Research Institute, Chinese Academy of Fishery Sciences.

The juvenile and adult Chinese giant salamanders were obtained from the Yangtze River Fisheries Research Institute, Chinese Academy of Fishery Sciences. And these animals were kept in aerated tap water at 20 ± 2 °C. Tissues (thymus, spleen, liver kidney, heart, brain and muscle) were obtained from three individual salamanders of each age group (4, 6, 9, 12, 14 and 17-month-old Chinese giant salamanders). All the salamanders were anesthetized using tricaine methane sulphonate (MS-222) (Sigma) before euthanasia.

2.2. RT-PCR, cloning and sequencing

Total RNA from every tissue was extracted immediately after sampling with TRIzol Reagent according to the manufacturer's instructions. In order to eliminate contaminating genomic DNA, the samples were DNase treated for 6 h and extracted by phenol/chloroform as previously described (Jiang et al., 2012). Reverse transcription of cDNA was performed according to the protocol of the ReverlAid First Stand cDNA Synthesis Kit (Thermo Scientific) as previously described (Jiang et al., 2015). The open reading frames of *rag1* and *rag2* were first determined by *de novo* transcriptome sequencing of Chinese giant salamander (Fan et al., 2015). Then, full length sequences were amplified from the spleen cDNA of 4-month-old salamanders by PCR using the specific primer, respectively (Table 1). After cloning in pMD19-T vector (TaKaRa), the *rag1* and *rag2* were sequenced to confirm the nucleotide identities. The complete ORF regions and amino acid sequences of *rag1* and *rag2* were deduced using ORF finder at National Center for Biotechnology Information (http://www.ncbi.nlm.nih.gov/gorf/gorf.html). Protein sequences of RAG1 and RAG2 from different species were used to perform multiple alignments using ClustalW2. Amino acid sequences of the RAG1 and RAG2 in other species were obtained from the NCBI GenBank database. The molecular phylogenetic tree was constructed by Molecular Evolution Genetics Analysis (MEGA) software version 3.1 using the neighbor-joining method (Kumar et al., 2004).

Table 1
Primers used in this study.

Primer	Sequence (5′-3′) Used for Amplicon size or reference
rag1 A	ATGGAGATTCCCCTGCCAGG Cloning 3153 bp
rag1 B	TCAGAATTCAACTGAATCTA
rag2 A	CCACCTTCTGCCATCCAGGT 1632 bp
rag2 B	GTCTTCTGTGAACCTGGCCC
rag1 RA	TGCACTGGTGTCCACCTTGA Real-time PCR 134 bp
rag1 RB	TGACATCTCCCATTCCGTCG
rag2 RA	GGGGACTCTGACGCAGAAGA 100 bp
rag2 RB	GATACACGGCGGACATGACA
18s F	CCTGAGAAACGGCTACCACATCC Yang et al., 2010
18s R	AGCAACTTTAGTATACGCTATTGGAG
rag1 PA	ATGACCATTGCGGTCCCTCA Probe synthesis 479 bp
rag1 PB	TCAATGAAGGGCTTGGCTGA
rag2 PA	TTCATCCCTGATACAGCCGG 557 bp
rag2 PB	GGATGTACGAGTTGGAGCATCC
igY PA	ACGGAAATGTGGCTTCCCT 562 bp
igY PB	AGTTCCAGCTGGTGTGGGG
tcr PA	GAAGGGCGCTGAGCATAGA 541 bp
tcr PB	CTGGCATTGTCCCTGGTGG

2.3. Quantitative real-time PCR

Quantitative real-time PCR was performed using the FastStart Universal SYBR Green Master (Roche Diagnostics, GmbH) to examine the expressions of *rag 1* and *rag 2*. Each real-time PCR program included the following procedures: 95 °C for 30 s, 95 °C for 15 s, 60 °C for 20 s and 72 °C for 35 s; Steps 2–4 were repeated for 40 cycles. All primers used for real-time PCR are listed in Table 1.

2.4. In situ hybridization

The *rag1*, *rag2*, *IgY* and *tcrβ* probes were synthesized using T7 RNA polymerase with a digoxygenin (DIG) RNA-labeling kit (Promega) following the manufacturer's procedures. The primers used in the preparation of the probes were showed in Table 1. For each gene, sense probes were used as negative control. Section *in situ* hybridization was performed as previously described (Jiang et al., 2015). 4% PFA-fixed tissues were dehydrated with 30% sucrose/PBS and then embedded in optimum cutting temperature compound (OCT, Leica, Germany). Transverse serial sections (8 μm) of each tissue were sectioned at −20 °C (UC7, Leica, Germany). The sections were rehydrated with PBS three times, and then the DIG-labeled probes were added to the sections and incubated overnight at 65 °C. The sections were incubated with anti- DIG antibody (1:4000; Roche Diagnostics, GmbH), and then stained with NBT/BCIP (Roche Diagnostics). The sections were examined with light microscopy with CCD picture system (DM2500, Leica, Germany).

2.5. Histology and HE staining

The transverse serial sections of thymus and spleen from 4 months to 17 months Chinese giant salamanders were rehydrated with PBS and stained with haematoxylin and eosin (HE). After dehydration through a graded series of ethyl-alcohol, cleared in xylene and sealed with neutralized resin, the sections were examined with light microscopy.

2.6. Statistical analysis

For the real-time PCR results, three replicates of each sample were expressed as means (± SD). The mRNA level of each gene in each sample was first calculated as the ratio with 18S ribosomal RNA transcript levels that were amplified as an internal control (Jiang et al., 2015) and then expressed as a fold-increase relative to the 4-month-old spleen sample. The data were analyzed by one-way ANOVA followed by the Dunnett test. A $p \leq 0.05$ was considered to be significant. The results were repeated three times.

3. Results

3.1. Characteristics of rag1 and rag2 open reading frame

The open reading frame sequences of *rag1* and *rag2* had been accessed with the numbers (MH106790 and MH106791, respectively). The *rag1* open reading frame consists of 3153 nucleotides that encods a 1051 amino acid protein (Supplementary Fig. 1), and the *rag2* open reading frame consistes of 1560 nucleotides that encodes a putative 520 amino acid protein (Supplementary Fig. 2). To infer the evolution relationships of *RAG1* and *RAG2* with those of other vertebrate species, a multiple alignment with other known deduced RAG1and RAG2 protein sequences was performed (Supplementary Fig. 1, Supplementary Fig. 2). The multiple sequence alignment of RAG1 and RAG2 showed the overall conservation of RAG1 and RAG2 sequences within vertebrates. The conserved amino acid residues of RAG1 were concentrated in the carboxy-terminal two-third of the protein (Supplementary Fig. 1). The dissimilarities of RAG2 amino acid sequence was distributed throughout the protein. In addition, a phylogenetic tree was constructed using the neighbor-joining method to evaluate the evolutionary relationship of RAG1 and RAG2, the *Andrias davidianus* RAG1 and RAG2 shared a closer relationship with *Xenopus laevis* RAG1 and RAG2, respectively (Fig. 1).

3.2. Expressions of rag1 and rag2

Real-time PCR results showed significant expression levels of *rag1* and *rag2* in the thymus, spleen, liver and kidney of 4- to 17-month-old salamanders. High expression levels of *rag1* and *rag2* were detected in the thymus during early development, and the expression levels remained at low but significant level in the thymus after 14 months. In the spleen, the *rag1* and *rag2* expression levels were much lower than thymus from 4 months to 14 months but remained significant. A low but significant and reproducible expression level of *rag1* and *rag2* was detected in the liver and kidney of 4- to 17-month-old salamanders (Fig. 2).

3.3. Detection of rag1, rag 2 transcription by in situ hybridization

To further substantiate *rag1* and *2* gene expression profiles by qPCR we performed ISH. Temporal and spatial expression patterns of *rag1* and *rag2* in the thymus, spleen, as well as the liver and kidney of 4- to 17-month-old Chinese giant salamanders were examined. In all gnathostomes, the thymus histogenesis can be divided into four sequential steps: the appearance of the thymus primordium, its colonization by lymphocyte precursors, the expansion of thymocytes and the histological regionalization of this gland (Castillo et al., 1990). The specific signals of *rag1* and *rag2* transcripts were detected at the periphery of the thymic primordium of 4-month-old salamanders (Fig. 3 A, G). In the thymus of 6-month-old salamanders, more *rag1* and *rag2* expression signals were detected mainly in the sub-capsular region of the thymus and fewer in the medulla (Fig. 3 B, H). From 9 months to 17 months, the signals of both *rag1* and *rag2* were randomly scattered throughout the entire thymus including cortex and medulla (Fig. 3 C-F, I-L). In the spleen, specific *rag1* and *rag2* signals were randomly scattered in the entire spleen of 4- to 17-month-old salamanders (Fig. 4A–L). Furthermore, *rag1* and *rag2*–positive cells were observed in the hepatic peripheral hematopoietic layer and in the vicinity of the blood vessel in 4-

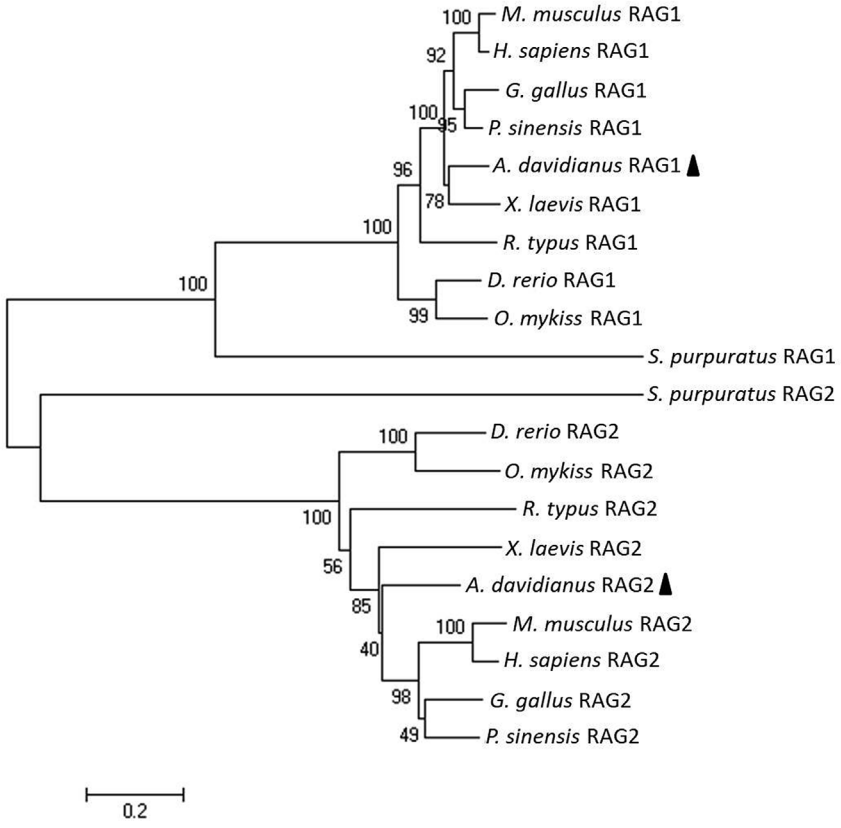

Fig. 1. Phylogenetic trees of RAG1and RAG2. The phylogenetic tree was constructed based on the full-length amino acid sequences by the Neighbor-joining method and the bootstrap value was set at 1000. The *Andrias davidianus* (*A. davidianus*) RAG1 and RAG2 are indicated with triangle (▲). Percentage of bootstrap replications is shown in the figure. The scale bar (0.2) represented the genetic distance. The accession numbers of the selected sequences are the same as those used for alignment. *Xenopus laevis* (*X. laevis*) RAG1 (NP_001165554.1), RAG2 (L19325.1); chicken (*G. gallus*) RAG1 (NP_001026359.1), RAG2 (NP_001291986.1); mouse (*M. musculus*) RAG1 (NP_033045.2), RAG2 (NP_033046.1); human (*H. sapiens*) RAG1 (NP_000439.1), RAG2 (NP_000527.2); zebrafish (*D. rerio*) RAG1 (NP_571464.1), RAG2 (NP_571460.2); rainbow trout (*O. mykiss*) RAG1 (NP_001118209.1), RAG2 (NP_021428825.1); sea urchin (*S. purpuratus*) RAG1 (NP_001028179.1), RAG2 (NP_001028184.1); Chinese soft-shelled turtle (*P. sinensis*) RAG1 (XP_006124532.1), RAG2 (XP_006124533.1); whale shark (*R. typus*) RAG1 (XP_020385577.1), RAG2 (XP_020385564.1).

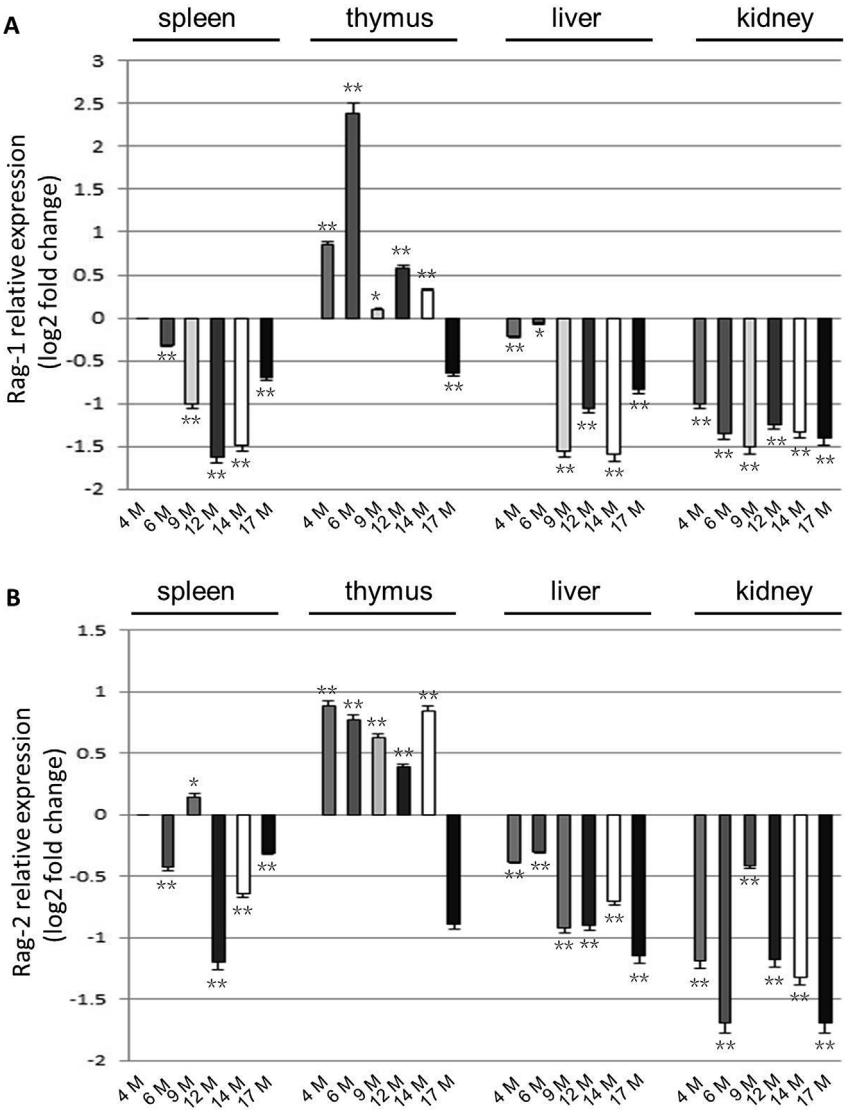

Fig. 2. Relative expressions (log2) of *rag1* (A) and *rag2* (B) genes in the spleen, thymus, liver and kidney of 4- to 17-month-old salamanders determined by real-time PCR. Expression of 18S ribosomal RNA was used as an internal control for real-time PCR. Positive and negative log2 expression ratios represent up- and down-regulation respectively. Each experiment was performed in triplicate. Deviation bars represented mean ± SD (n = 3). The significant differences were indicated with asterisks, *p ≤ 0.05; **p ≤ 0.01.

to 17-month-old salamander livers (Fig. 5). Similarly, the *rag1* and *rag2* signals were detected in the peripheral layer of the kidney of 4- to 17-month-old salamanders (Fig. 6). Importantly, no *rag1* and *rag2* signal was detected either in the thymus, spleen, liver or kidney when labeled with sense *rag1* or *rag2* probes used as negative controls (Supplementary Fig. 3). The relatively scant detection of cells expressing *rag1* and *rag2* may be due to the sensitivity of the ISH.

3.4. Detection of igY and tcrβ transcription by in situ hybridization

The expression of *igY* and *tcrβ* were used as indicator of differentiate B and T cells. The expression pattern of *igY* and *tcrβ* were similar with *rag1* and *rag2* in the thymus, spleen, liver and kidney (Fig. 7). Both *igY* and *tcrβ* specific signals were distributed at the periphery of the thymus primordium of 4-month-old salamander and at the cortical region of the thymus of 6-month-old salamanders (Fig. 7 A, B, D, E); then became randomly scattered in the entire thymus of 17-month-old salamanders (Fig. 7 C, F). In the spleen of 6-month-old salamanders, *igY* and *tcrβ* signals were randomly scattered in the whole organ (Fig. 7 G, H); whereas in the liver they were localized in the hepatic peripheral hematopoietic layer and in the vicinity of the blood vessel (Fig. 7 I, J). *Tcrβ* signals were observed at the periphery of the kidney of 14-month-old salamanders (Fig. 7 L). In contrast, *igY*-specific signals were observed not only at the periphery but also at the hematopoietic tissue of the kidney of 14-month-old salamanders (Fig. 7 K). No *igY* or *tcr* signal was detected in thymus, spleen, liver or kidney when labeled with sense *igY* or *tcr* probes (Supplementary Fig. 3). Although one would expect a higher frequency of *igY* and *tcr* expressing cells, it is probable that the sensitivity our ISH was insufficient to detect cell with low levels of *igY* and *tcr* transcripts.

3.5. Histological analysis of thymus and spleen organogenesis

To complement our ISH study, change in morphology of thymus and spleen of 4- to 17-month-old salamanders was examined by conventional histology (Figs. 8 and 9). The transverse sections of the thymus of 4-month-old and 6 -month-old salamanders were made at a level posterior to the eye and anterior to the inner ear through the hindbrain region. The branched thymic primordium was located in the deep muscles in the pharyngeal region of 4-month-old salamanders (Fig. 8A

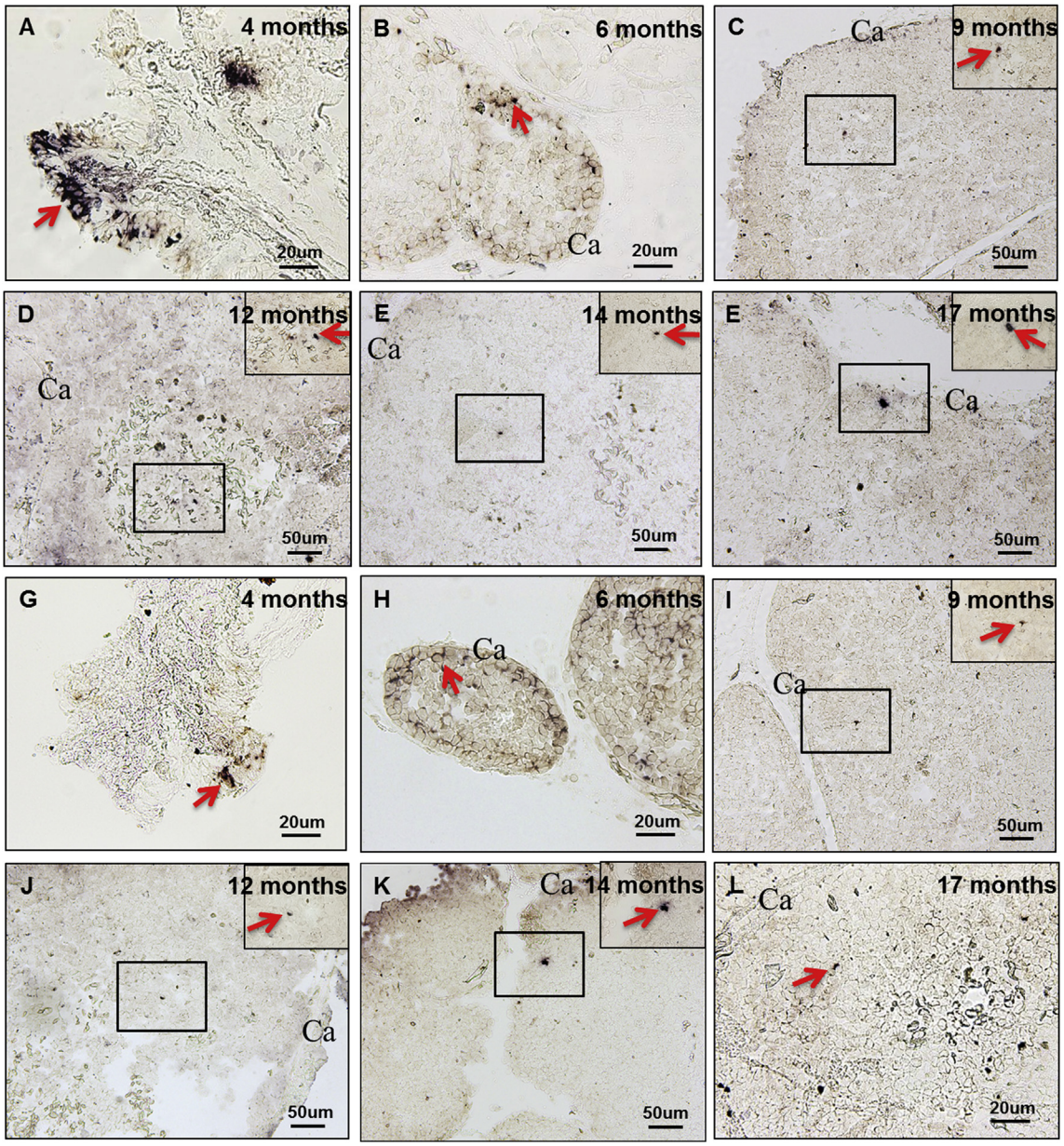

Fig. 3. Developmental expression of *rag1* and *rag2* in the thymus of 4- to 17-month-old salamanders determined by *in situ* hybridization. *Rag1* (A) and *rag2* (G) expressions at 4 months were detected mainly at the epithelial layer of thymic primordium. *Rag1* (B) and *rag2* (H) expressions at 6 months were detected mainly at the edge of thymus. *Rag1* (C- F) *and rag2* (I- L) expressions from 9 months to 14 months were showed randomly scattered in the entire thymus. Arrows indicated the positive signals. Ca: capsula. Transverse sections (A, B, G, H) through the hindbrain region at a level posterior to the eye and anterior to the inner ear. Scale bar (A, B, G, H, L) = 20 μm, scale bar (C- E, I- K) = 50 μm.

and B). As development proceeded, the thymic primordium of 6-month-old salamanders was translocated toward the skin, and became round in shape (Fig. 8 C, D). Meanwhile, thymus arterioles were formed at 6 months (Fig. 8 C, D) when lymphocytes were detected by ISH. The thymocytes had expanded and differentiated into cells of different size and morphology and the whole organ size increased concomitant with the growth from 6 months to 17 months (Fig. 8C–H). The Hassall's corpuscles were detected in the medulla at 6 months of age (Fig. 8C–H). The thymus capsula was also detected at 6 months and thymic lobes were partly separated by trabeculae at 9 months of age (Fig. 8C–H). Compared to early stage of development (4-month old), the spleen of 17-month-old Chinese giant salamanders showed increased number of splenocytes and enlarged organ size (Fig. 9). Lymphocytes were found spread over the whole spleen without a distinguishable delimitation between the red and white pulp. Lymphocytes were preferentially distributed in the vicinity of the blood vessel, and many blood sinuses were also observed among the lymphocyte (Fig. 9).

4. Discussions

RAG 1 and 2 proteins are required for mediating recombination of B and T cell receptors during lymphocyte development. As such the expression of these genes can be used as reliable indicator of lymphocyte differentiation in lymphopoietic tissues. In the present study, we characterized the full length coding sequences of the Chinese giant salamander *rag1* and *rag 2* gene homologs sharing a close phylogenetic relationship with their respective *Xenopus RAG1* and *RAG2* homologs (Fig. 1). Moreover, the consensus of amino acid sequence of RAG1 was mainly concentrated in the carboxy-terminal two-third of the protein compared to other species (Supplementary Fig. 1), which indicated

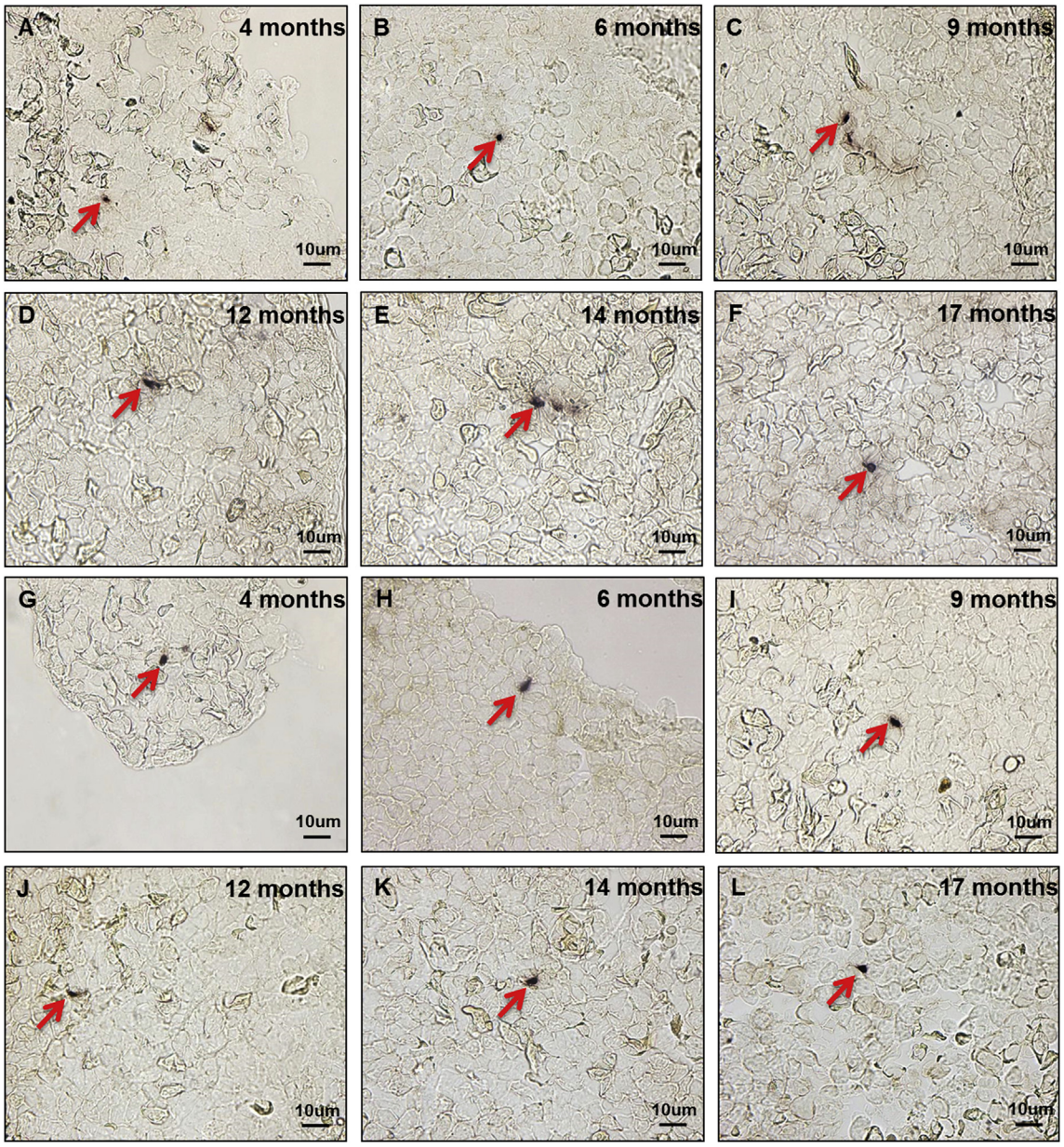

Fig. 4. Developmental expression of *rag1* and *rag2* in the spleen of 4- to 17-month-old salamanders determined by *in situ* hybridization. *Rag1* (A–F) *and rag2* (G–L) specific signals were detected randomly scattered throughout the entire spleen. Arrows indicated the positive signals. Scale bar = 10 μm.

strongly conserved throughout evolution and essential for *ig* and *tcr* genes rearrangement as in zebrafish, *Pleurodeles waltl* (Willett et al., 1997; Frippiat et al., 2001) and *Xenopus* (Greenhalgh et al., 1993). The active domain of RAG2 had been defined as the amino-terminal three-quarters of the protein (Willett et al., 1997), while the conservation of RAG2 was not limited to the active domain (Supplementary Fig. 2).

As an indirect way to identify tissue sites supporting B and T lymphocyte differentiation in the Chinese giant salamander at different stage of development, we monitored the co-expression *rag1* and *rag2* in combination with *igY* and *tcrβ* genes. Mammalian lymphocytes arise from hematopoietic precursors, and then these precursors cells differentiate in the liver and bone marrow for B cells and the thymus for T cells (Durand et al., 2000).

4.1. B cell differentiation

The site for B cell differentiation in cold blooded vertebrates varies across species and does not occur in the bone marrow that is no hematopoietic. The bone marrow in *Xenopus* adults is the site of differentiation/storage of granulocyte including the final differentiation step of macrophage precursors (Grayfer and Robert, 2013); but in the absence of *rag* activity it does not support lymphopoiesis (Du Pasquier et al., 2000). However, multiple other amphibian anuran species utilize their bone marrow towards hematopoiesis (Yaparla et al., 2016). We were unable to detect any *rag1* and *2* transcripts in the bone marrow of 5-month-old Chinese giant salamanders by qPCR (data not showed in this paper). More future work needs to be performed to clarify the function of bone marrow of Chinese giant salamander. The expression patterns of *rag1*, *rag2* and *igY* suggested that the spleen, liver and kidney serve as sites of B cell differentiation in Chinese giant salamander (Figs. 4–7). In most fish, B cells differentiate in kidney, whereas in urodels such as axolotl they differentiate mainly in the spleen (Trede and Zon, 1998; Durand et al., 2000). In *Xenopus*, B cell differentiated in the liver and the spleen and therefore *rag* activity and rearrangement of *ig* gene were detected (Robert and Ohta, 2009). Liver is considered to be a transitory lymphopoietic tissue in the Mexican axolotl, and *rag1* signal

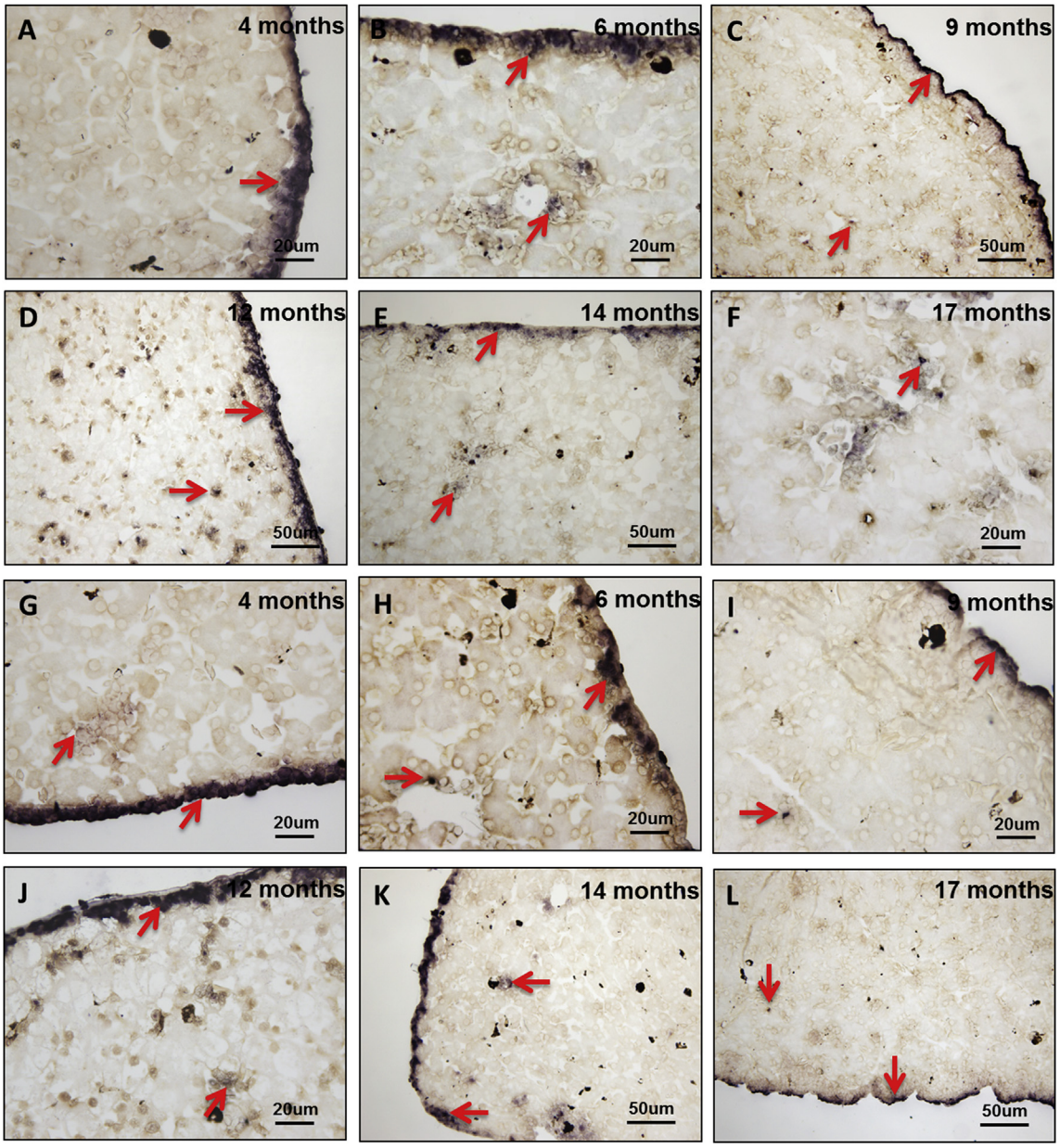

Fig. 5. Developmental expression of *rag1* and *rag2* in the liver of 4- to 17-month-old salamanders determined by *in situ* hybridization. *Rag1* (A–F) *and rag2* (G–L) specific signals were detected at the hepatic peripheral hematopoietic layer and in the vicinity of the blood vessel. Arrows indicated the positive signals. Scale bar (A, B, F- J) = 20 μm, scale bar (C-E, K, L) = 50 μm.

has been detected at the hematopoietic layer (Durand et al., 2000). In Chinese giant salamander, the *rag1* signals were not only detected in the hematopoietic layer but also in the vicinity of the blood vessel in liver (Fig. 5). In rainbow trout, *rag1* was expressed at moderate levels in adult spleen, indicated that B cells developed in spleen (Hansen, 1997). Kidney is a lymphopoietic tissue supporting B cell differentiation in zebrafish and trout (Willett et al., 1997), and *igM* positive cells have been observed at the kidney of turbot (Fournier-Betz et al., 2000). Beside kidney, the expression of *rag1* and *igu* transcripts was reported in the pancreas, suggesting that B cells also develop in the zebrafish pancreas (Danilova and Steiner, 2002). In Chinese giant salamander, lymphocytes differentiation located at the periphery layer of the kidney where the *rag1*, *rag2* and *igY* positive cells were observed (Figs. 6 and 7). *IgY* positive cells were observed in the kidney marrow while no *rags* positive cells was detected (Figs. 6 and 7K), it is difficult to rule out possible detection of these cells from the blood circulation.

The white pulp is defined as an organized lymphoid structure in spleen of mammals and salmonid (Ruddle and Akirav, 2009; Koppang et al., 2010). In *Xenopus*, the white pulp of the spleen is delimited from the red pulp by a two-cell layer of elongated cells termed the Grenzschichtmembran of Sterba (Manning and Horton, 1969). Large focal aggregates of lymphocytes organized as white pulp that contained a central artery, and erythrocytes and leukocytes in the red pulp surrounded white pulp (Bricker et al., 2012). In contrast to *Xenopus*, no obvious distinctive red pulp or white pulp was observed in Chinese giant salamander spleen, the lymphocyte spread over the whole spleen. Although more lymphocyte appeared in the vicinity of the blood vessel, the blood sinuses were observed among the lymphocyte (Fig. 9). Similar lack of distinctive red and white pulp in the spleen of flounder and cobia has been reported (Liu et al., 2004; Klosterhoff et al., 2015).

4.2. T cell differentiation

Thymus is the primary site of T cell differentiation for all jawed

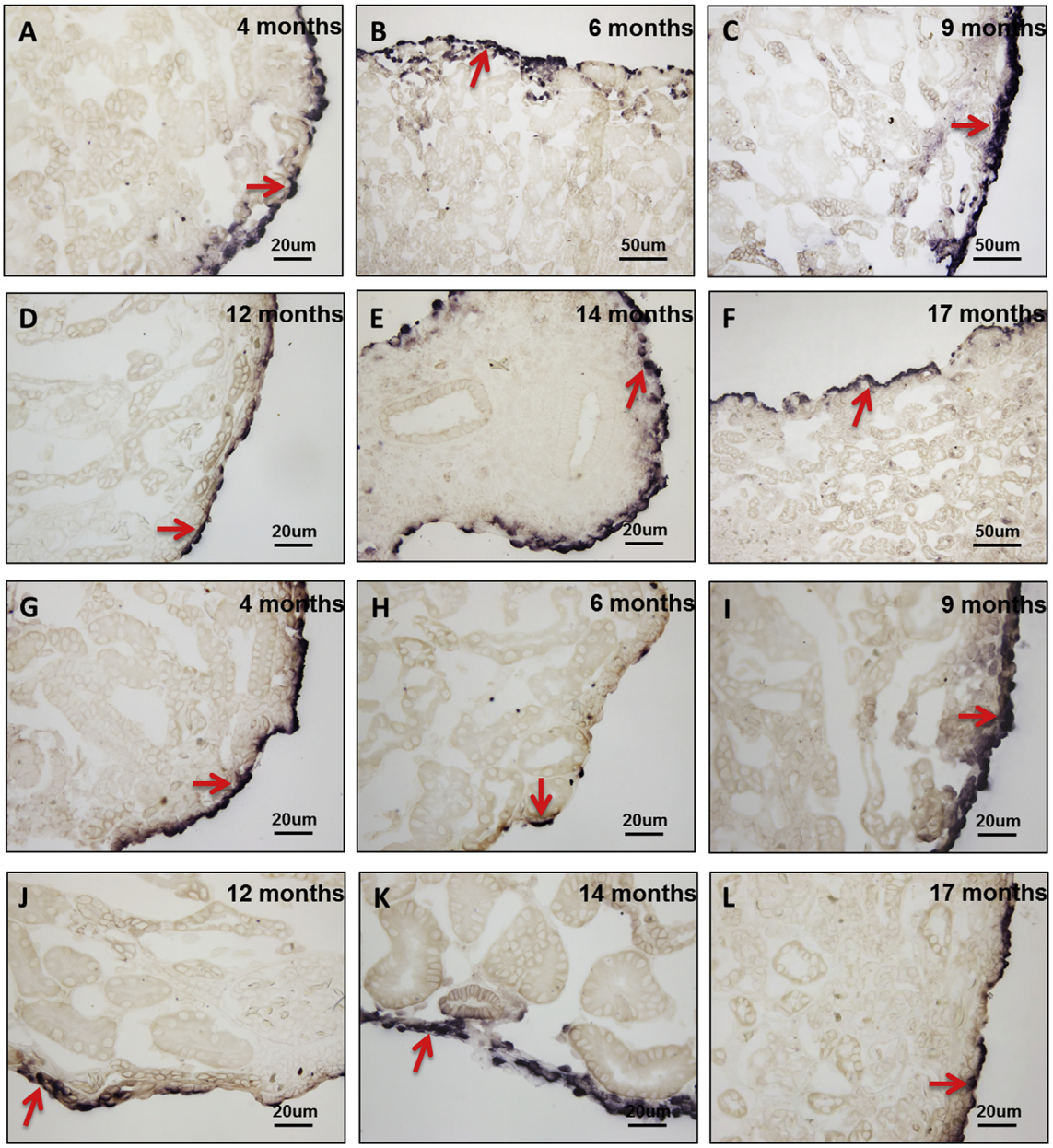

Fig. 6. Developmental expression of *rag1* and *rag2* in the kidney of 4- to 17-month-old salamanders determined by *in situ* hybridization. *Rag1* (A–F) *and rag2* (G–L) specific signals were detected only at the periphery of the tissue. Arrows indicated the positive signals. Scale bar (A, D, E, G- L) = 20 μm, scale bar (B, C, F) = 50 μm.

vertebrates (Gordon and Manley, 2011). In *Xenopus* it has been shown to be required for T cell differentiation, and not surprisingly *rag1* and *rag2* are both expressed at high levels (Greenhalgh et al., 1993; Robert et al., 2002). In Chinese giant salamander, the expression levels of *rag1* and *rag2* were much higher in juvenile thymus than other tissues (Fig. 2), which is similar to *Pleurodeles*, Mexican axolotl, *Xenopus*, zebrafish and trout (Greenhalgh et al., 1993; Willett et al., 1997; Durand et al., 2000; Frippiat et al., 2001). In *Xenopus*, the thymus anlage appears at 3 days post-fertilization (dpf), the cortex-medulla architecture distinguished at 6–8 dpf and the thymus colonization by precursors followed by thymocytes differentiation occurs at 5–7 dpf (Robert and Cohen, 1998; Robert and Edholm, 2014). During metamorphosis, most thymocytes died and are replaced by new stem cells that differentiated into new adult T lymphocytes distinct from tadpole ones (Du Pasquier and Flajnik, 1990; Robert and Edholm, 2014). In urodele, which undergoes incomplete metamorphosis, the thymic pharyngeal buds are colonized by lymphoid precursor cells a few days after hatching (3–4 weeks), and then these cells spread in the surrounding mesenchyme and directly invade the thymus epithelial anlages via their peripheral basal layer (Durand et al., 1999). These immature thymocytes remain in the sub-capsular region of the thymus and differentiate in a centripetal manner (Durand et al., 1999). In Chinese giant salamander, thymocyte differentiation was found to occur later than *Xenopus* and other urodeles. Both *rag1* and *rag2* transcripts were detected at the periphery of the thymus primordium of 4-month-old salamanders where immature thymocytes undergo differentiation. At later developmental stages (6 months of age) *rag* transcripts became more widely distributed throughout the cortical region of the thymus (Fig. 3). *Rag1* and *rag2* expressions in these areas imply the occurrence of lymphocyte, presumably T cell receptor recombination. However, the co-expression of *igY* besides *tcrβ* detected in juvenile and adult thymus by ISH (Fig. 7) suggests that the thymus harbor differentiated B cells. Although it is difficult to rule out possible detection of differentiated B and T cells from the blood circulation, the widespread and

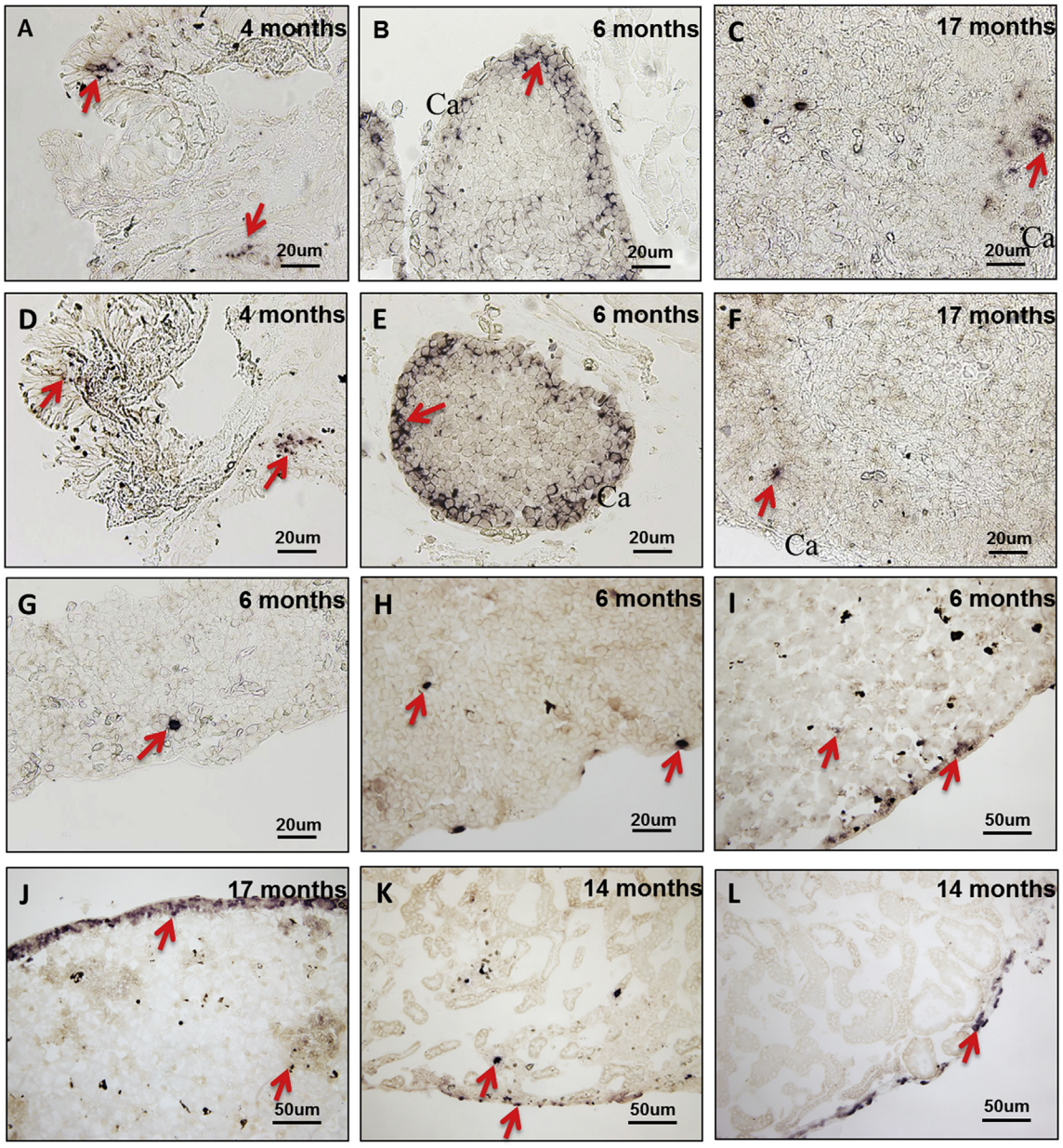

Fig. 7. Developmental expression of *igY* and *tcrβ* by *in situ* hybridization. A–C: *IgY* expression in the thymus of 4-, 6-, and 17-month-old salamanders. D–F: *Tcrβ* expression in the thymus of 4-, 6-, and 17-month-old salamanders. G: *IgY* expression in the spleen of 6-month-old salamanders. H: *Tcrβ* expression in the spleen of 6-month-old salamanders. I: *IgY* expression in the liver of 6-month-old salamanders. J: *Tcrβ* expression in the liver of 6-month-old salamanders. K: *IgY* expression in the kidney of 14-month-old salamanders. L: *Tcrβ* expression in the kidney of 14-month-old salamanders. Arrows indicated the positive signals. Ca: capsula. Scale bar (A–H) = 20 μm, Scale bar (I- L) = 50 μm.

scattered distribution of *tcr* and *ig* positive cells in the whole tissue would suggest that in the Chinese giant salamander juvenile and adult thymus in addition to be a major site for T cell differentiation can also serve as a secondary site for B cells. Similar observation has been reported for *Xenopus* in early literature (Du Pasquier and Weiss, 1973). Although *rag1*, *rag2* and *tcrβ* transcription signals were detected in the spleen, liver and kidney (Figs. 4–7), it's hard to prove T cell differentiation in these tissues because *tcrβ* transcription could also be detected in mature T cells. The mature T cells which have differentiated in the thymus could migrate through blood circulation and stored in the kidney of zebrafish and spleen of *Xenopus* (Langenau et al., 2004; Robert and Ohta, 2009).

The location of thymus could range from the proximity of the thyroid to underneath strings of muscle in mammals, but the thymus does not migrate in birds and fish throughout their lives (Ge and Zhao, 2013). Similar to mammals, the thymus primordium of Chinese giant salamander initially develop at a deep position in the pharyngeal muscles, and then translocated towards the skin (Fig. 8), which is similar to *Xenopus laevis* (Lee et al., 2013). The thymus developed to form a unique microenvironment critical for supporting T cell maturation and regeneration (Gordon and Manley, 2011). Hassall's corpuscles, which were found in the medulla of the thymus of mammals, are derived from lymphoepithelial cells connected by desmosomes. These cells, especially those in the center of the organ, could degenerate and die, leaving cellular debris that may calcify (Klosterhoff et al., 2015). In 6 months in Chinese giant salamander, Hassall's corpuscles structurally, similar to that of mammals, were found in thymic medulla in parallel with the detection of thymic arterioles and the developmental lymphocyte expressing *rag1* and *rag2* (Figs. 3 and 8). Hassall's corpuscles may be involved in lymphocyte development of Chinese giant

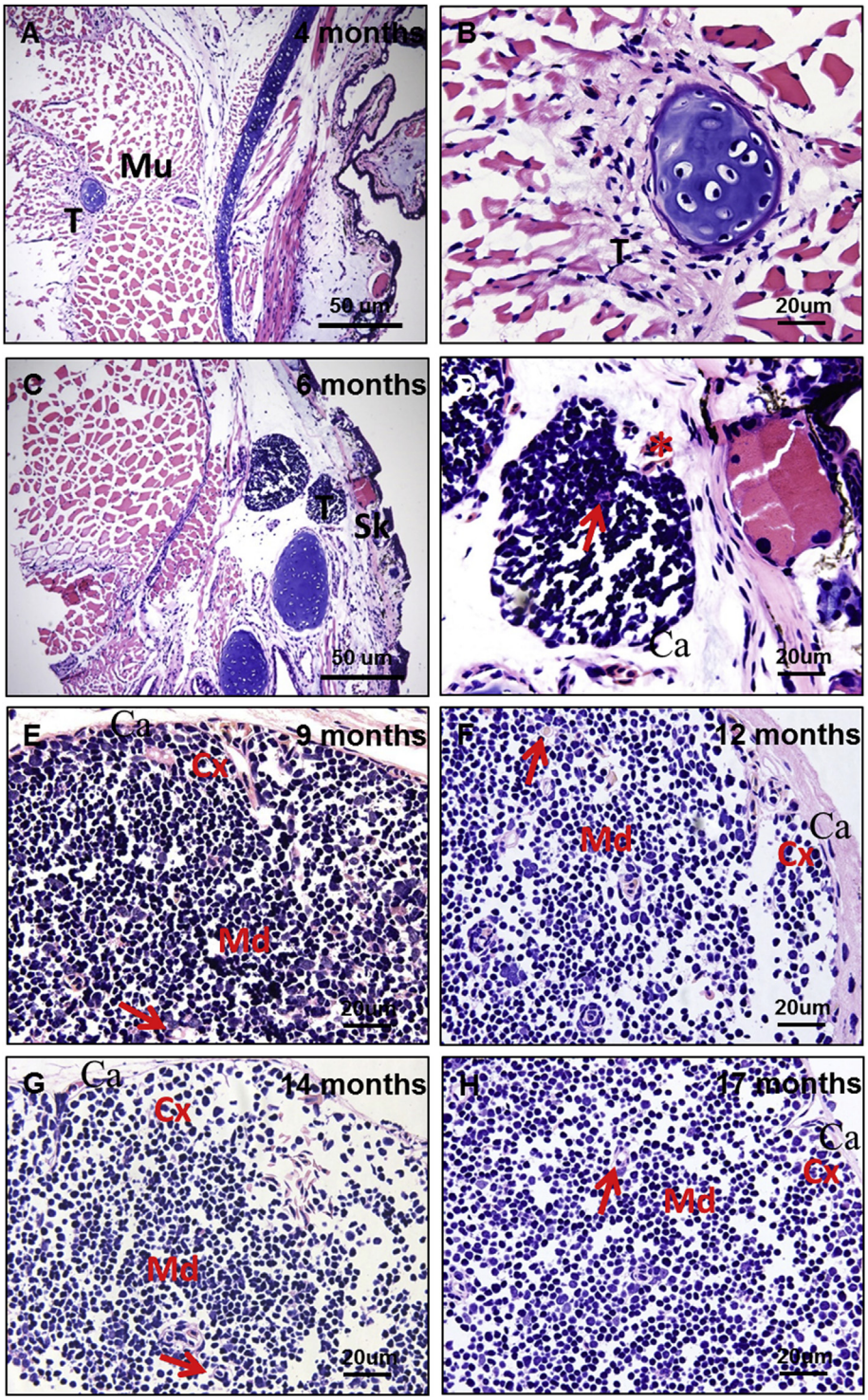

Fig. 8. Histological sections stained with hematoxylin and eosin of the Chinese giant salamander thymus during development from 4 months to 17 months of age. A: Thymic primordium (T) embedded in the muscles (Mu) at 4 months. B: Higher magnification of thymic primordium depicted in A. C: Thymus (T) located under skin (Sk) at 6 months of age. D: Higher magnification of thymus depicted in C; arrows indicate Hassall's corpuscles and asterisks indicate arterioles. E–H: Thymus increased in size from 9 months to 17 months; arrows indicate Hassall's corpuscles. Ca: capsula, Cx: cortex, Md: medulla. Transverse sections (A–D) through the hindbrain region at a level posterior to the eye and anterior to the inner ear. Scale bar (A, C) = 50 μm, (B, D, E-H) = 20 μm. Sections were stained with HE.

salamander, and the matured T cells would exit from the thymus through the thymus arterioles. The axolotl thymus had no clear cortex-medulla histological compartmentalization, which is different from chicken and *Xenopus* (Tournefier et al., 1990). Also, there was no significantly distinction between cortex and medulla in Chinese giant salamander. According to histological analysis, we considered the areas containing the trabeculae as cortex, whereas the area containing the Hassall's corpuscles as medulla (Fig. 8). The anatomical organization of the salmonid thymic cortex and medulla seems to be composed of three layers through anti-CD3 immunostaining (Koppang et al., 2010). Whether the Chinese giant salamander thymus exhibit similar layers and whether there is a distinctive cortex-medulla remains to be determined.

In conclusion, Chinese giant salamander *rag1* and *rag2* gene homologs closely related to *Xenopus laevis rag1* and *rag2*, respectively, have been characterized. The high expression levels of both *rag1* and *rag2* were used as proxy to detect lymphocyte differentiation in the thymus as early as 14 months. The spatial co-expression patterns of *rag1*, *rag2*, *igY* and *tcrβ* determined by ISH suggests that besides the thymus and spleen, liver and kidney can serve as lymphopoietic tissues supporting lymphocyte receptor rearrangement of presumably B cells and possibly T cells in the Chinese giant salamander.

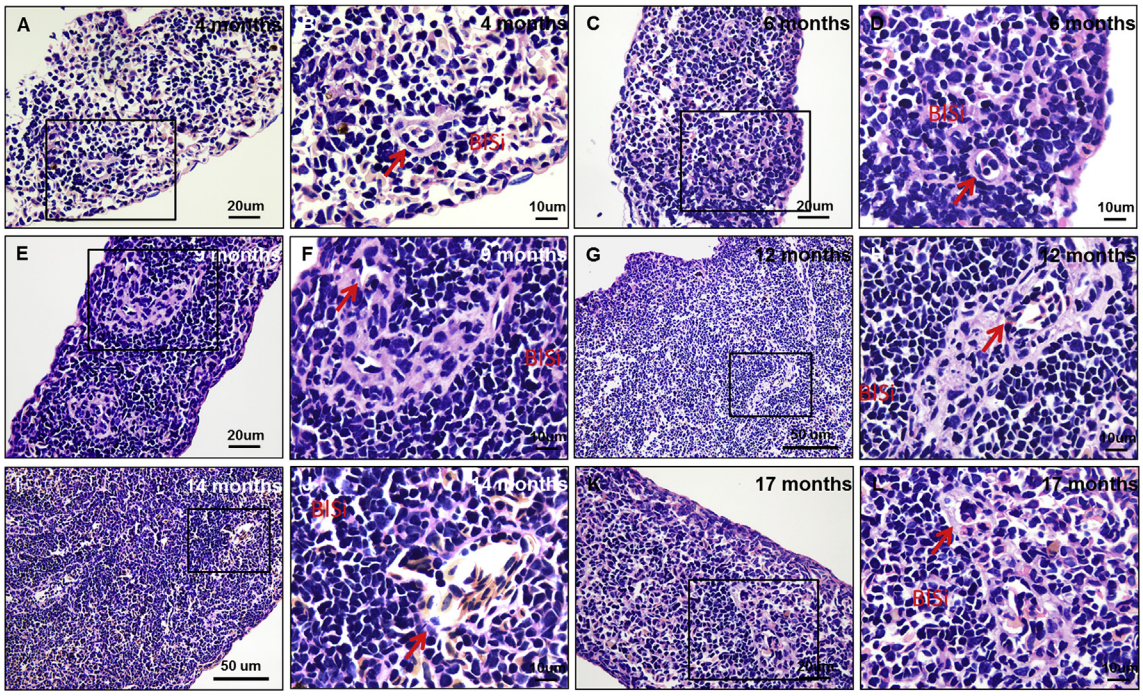

Fig. 9. Histological section stained with hematoxylin and eosin of the Chinese giant salamander spleen during development from 4 months to 17 months of age. A, C, E, G, I, K: Spleen of 4- to 17-month-old salamanders. B, D, F, H, J, L: Higher magnification of the spleen of 4- to 17-month-old salamanders. Arrows indicate blood vessels. BlSi: blood sinuses. Scale bar (A, C, E, K) = 20 μm, (B, D, F, H, J, L) = 10 μm. (G, I) = 50 μm. Sections were stained with HE.

Acknowledgements

The work was supported by the National Natural Science Foundation of China (Grant No. 31702033) and the Special Fund for Agro-Scientific Research in the Public Interest (201203086-05).

Appendix A. Supplementary data

Supplementary data related to this article can be found at http://dx.doi.org/10.1016/j.dci.2018.05.018.

References

Bricker, N.K., Raskin, R.E., Densmore, C.L., 2012. Cytochemical and immunocytochemical characterization of blood cells and immunohistochemical analysis of spleen cells from 2 species of frog, *Rana (Aquarana) catesbeiana* and *Xenopus laevis*. Vet. Clin. Pathol. 3, 353–361.

Castillo, A., Razquin, B.E., Lopez-Fierro, P., Alvarez, F., Zapata, A., Villena, A.J., 1990. Enzyme- and immnno-histochemical study of the thymic stroma in the rainbow trout, *Solmo jairdneri* Richardson. Thymus 36, 159–173.

Chen, Z., Gui, J., Gao, X., Pei, C., Hong, Y., Zhang, Q., 2013. Genome architecture changes and major gene variations of *Andrias davidianus* ranavirus (ADRV). Vet. Res. 44, 101.

Danilova, N., Steiner, L.A., 2002. B cells develop in the zebrafish pancreas. Proc. Natl. Acad. Sci. U.S.A. 99, 13711–13716.

Dong, W., Zhang, X., Yang, C., An, J., Qin, J., Song, F., Zeng, W., 2011. Iridovirus infection in Chinese giant salamanders, China. Emerg. Infect. Dis. 17, 2388–2389.

Du Pasquier, L., Weiss, N., 1973. The thymus during the ontogeny of the toad Xenopus laevis: growth, membrance-bound immunoglobulins and mixed lymphocyte reaction. Eur. J. Immunol. 3, 773–777.

Du Pasquier, L., Flajnik, M.F., 1990. Expression of MHC class II antigens during Xenopus development. Dev. Immunol. 1, 85–95.

Du Pasquier, L., Robert, J., Courtet, M., Mussmann, R., 2000. B-cell development in the amphibian *Xenopus*. Immunol. Rev. 175, 201–213.

Durand, C., Charlemagne, J., Fellah, J.S., 1999. Structure and developmental expression of *Ikaros* in the Mexican axoloti. Immunogenetics 50, 336–343.

Durand, C., Charlemagne, J., Fellah, J.S., 2000. *RAG* expression is restricted to the first year of life in Mexican axoloti. Immunogenetics 51, 681–687.

Fan, Y., Chang, M.X., Ma, J., Scott, E.L., Hu, Y.W., Huang, L., Nie, P., Zeng, L., 2015. Transcriptomic analysis of the host response to an iridovirus infection in Chinese giant salamander, *Andrias davidianus*. Vet. Res. 46, 126–156.

Fellah, J.S., Kerfourn, F., Wiles, M.V., Schwager, J., Charlemagne, J., 1993. Phylogne of immunoglobulin heavy chain isotypes: structure of the constant region of Ambystoma mexicanum upsilon chain deduced from cDNA sequence. Immunogenetics 38, 311–317.

Fournier-Betz, V., Quentel, C., Lamour, F., Leven, A., 2000. Immunovytochemical detection of Ig-positive cells in blood, lymphoid organs and the gut associated lymphoid tissue of the turbot (*Scophthalmus maximus*). Fish Shellfish Immunol. 10, 187–202.

Frippiat, C., Kremaril, P., Ropars, A., Dournon, C., Frippiat, J., 2001. The recombination activation genes 1 of *Pleurodeles waltl* (urodele amphibian) is transcribed in lymphoid tissues and in the central never system. Immunogenetics 52, 264–275.

Ge, Q., Zhao, Y., 2013. Evolution of thymus organogenesis. Dev. Comp. Immunol. 39, 85–90.

Geng, Y., Wang, K.Y., Zhou, Z.Y., Li, C.W., Wang, J., He, M., Yin, Z.Q., Lai, W.M., 2011. First report of a ranavirus associated with morbidity and mortality in farmed Chinese giant salamanders (*Andrias davidianus*). J. Comp. Pathol. 145, 95–102.

Gordon, J., Manley, N.R., 2011. Mechanisms of thymus organogenesis and morphogenesis. Development 138, 3865–3878.

Grayfer, L., Robert, J., 2013. Colony- stimulating factor-1-responsive macrophage precursors reside in the amphibian (*Xenopus laevis*) bone marrow rather than the hematopoietic sub-capsular liver. J. Innate. Immun 5, 531–542.

Greenhalgh, P., Olesen, C.E., Steiner, L.A., 1993. Characterization and expression of recombination activating genes (*RAG-1* and *RAG-2*) in *Xenopus laevis*. J. Immunol. 151, 3100–3110.

Gui, L., Chinchar, V.G., Zhang, Q., 2018. Molecular basis of pathogenesis of emerging viruses infecting aquatic animals. Aquacult. Fish 3, 1–5.

Hansen, J.D., 1997. Characterization of rainbow trout terminal deoxynucleotidyl transferase structure and expression. TdT and rag1 co-expression define the trout primary lymphoid tissues. Immunogenetics 46, 367–375.

Hansen, J.D., Zapata, A.G., 1998. Lymphocyte development in fish and amphibians. Immunol. Rev. 166, 199–220.

Huttenhuis, H.B.T., Huising, M.O., van der Meulen, T., van Oosterhoud, C., SCnchez, N.A., Taverne-Thiele, A.J., Stroband, H.W.J., Rombout, J.H.W.M., 2005. *Rag* expression identifies B and T cell lymphopoietic tissues during the development of common carp (*Cyprinus carpio*). Dev. Comp. Immunol. 29, 1033–1047.

Ijspeert, H., Driessen, G.J., Moorhouse, M.J., Hareig, N.G., Wolska-Kusnierz, B., Kalwak, K., Pituch-Noworolska, A., Kondratenko, I., van Montfrans, J.M., Mejstrikova, E., Lankester, A.C., Langerak, A.W., van Gent, D.C., Stubbs, A.P., van Dongen, J.J.M., van der Burg, M., 2014. Similar recombination-activation gene (*RAG*) mutations results in similar immunobiological effects but in different clinical phenotypes. J. Allergy Clin. Immunol. 133, 1124–1133.

Jiang, N., Jin, X., He, J., Yin, Z., 2012. The role of follisatin 1 in regulation of zebrafish fecundity and sexual differentiation. Biol. Reprod. 87, 54.

Jiang, N., Fan, Y., Zhou, Y., Liu, W., Ma, J., Meng, Y., Xie, C., Zeng, L., 2015. Characterization of Chinese giant salamander iridovirus tissue tropism and inflammatory response after infection. Dis. Aquat. Org. 114, 229–237.

Kaufman, J., Skjoedt, K., Salomonsen, J., 1990. The MHC molecules of nonmammalian vertebrates. Immunol. Rev. 113, 83–117.

Kerfourn, F., Charlemagne, J., Fellah, J.S., 1996. The structure, rearrangements and ontogenic expression of *DB* and *JB* genes segments in the Mexican axolotl T-cell receptor beta chain (*TCRB*). Immunogenetics 44, 275–285.

Klosterhoff, M.C., Júnior, J.P., Rodrigues, R.V., Gusmão, E.P., Sampaio, L.A., Tesser, M.B., Romano, L.A., 2015. Ontogenic development of kidney, thymus and spleen and phenotypic expression of CD3 and CD4 receptors on the lymphocytes of cobia (*Rachycentroncanadum*). An. Acad. Bras. Cienc 87, 2111–2121.

Koppang, E.O., Fischer, U., Moore, L., Tranulis, M.A., Dijkstra, J.M., Köllner, B., Aune, L., Jirillo, E., Hordvik, I., 2010. Salmonid T cells assemble in the thymus, spleen and in novel interbranchial lymphoid tissue. J. Anat. 217, 728–739.

Kumar, S., Tamura, K., Nei, M., 2004. MEGA3: integrated software for molecular evolutionary genetics analysis and sequence alignment. Briefings Bioinf. 5, 150–163.

Langenau, D.M., Ferrando, A.A., Traver, D., Kutok, J.L., Hezel, J.D., Kanki, J.P., Zon, L.I., Look, A.T., Trede, N.S., 2004. *In vivo* tracking of T cell development, ablation, and engraftment in transgenic zebrafish. Proc. Natl. Acad. Sci. U. S. A. 101, 7369–7374.

Lee, Y., Williams, A., Hong, C., You, Y., Senoo, M., Saint-Jeannet, J., 2013. Early development of the thymus in *Xenopus laevis*. Dev. Dynam. 242, 164–178.

Liu, Y., Zhang, S., Jiang, G., Yang, D., Lian, J., Yang, Y., 2004. The development of the lymphoid organs of flounder, *Paralichthys olivaceus*, from hatching to 13 months. Fish Shellfish Immunol. 16, 621–632.

Manning, M.J., Horton, J.D., 1969. Histogenesis of lymphoid organs in larvae of the South African clawed toad, *Xenopus laevis* (Daudin). J. Embryol. Exp. Morphol. 22, 265–277.

Meng, Y., Ma, J., Jiang, N., Zeng, L., Xiao, H., 2014. Pathological and microbiological findings from mortality of the Chinese giant salamander (*Andrias davidianus*). Arch. Virol. 159, 1403–1412.

Mombaerts, P., Iacoraini, J., Johnson, R.S., Herrup, K., Tonegawa, S., Papaioannou, V.E., 1992. RAG-1 deficient mice have no mature B and T lymphocytes. Cell 68, 869–877.

Robert, J., Cohen, N., 1998. Ontogeny of CTX expression in Xenopus. Dev. Comp. Immunol. 22, 605–612.

Robert, J., Gantress, J., Rau, L., Bell, A., Cohen, N., 2002. Minor histocompatibility antigen-specific MHC-restricted CD8 T cell responses elicited by heat shock proteins. J. Immunol. 168, 1697–1703.

Robert, J., Ohta, Y., 2009. Comparative and developmental study of the immune system in *Xenopus*. Dev. Dynam. 238, 1249–1270.

Robert, J., Edholm, E., 2014. A prominent role for invariant T cells in the amphibian *Xenopus laevis* tadpoles. Immunogenetics 6, 513–523.

Ruddle, N.H., Akirav, E.M., 2009. Secondary lymphoid organs: responding to genetic and environmental cues in ontogeny and immune response. J. Immunol. 183, 2205–2212.

Shinkai, Y., Rathbun, G., Lan, K.P., Oltz, E.M., Stewart, V., Mendelsohn, M., Charron, J., Datta, M., Young, F., Stall, A.M., 1992. RAG-2 deficient mice lack mature lymphocytes owing to inability to initiate V(D)J rearrangement. Cell 68, 855–867.

Trede, N.S., Zon, L.I., 1998. Development of T-cell during fish embryogenesis. Dev. Comp. Immunol. 22, 253–263.

Tournefier, A., 1975. Incomplete antibodies and immunoglobulin characterization in adult urodeles, *Pleurodeles waltlii* Michah, and *Triturus alpsetris* Laur. Immunology 29, 209–217.

Tournefier, A., Lesourd, M., Gounon, P., 1990. The axolotl thymus: cell types of the microenvironment. Cell Tissue Res. 262, 387–396.

Willett, C.E., Cherry, J.J., Steiner, L.A., 1997. Characterization and expression of the recombination activating genes (*rag1* and *rag2*) of zebrafish. Immunogenetics 45, 394–404.

Yang, L., Meng, Z., Liu, Y., Zhang, Y., Liu, X., Lu, D., Huang, J., Lin, H., 2010. Growth hormone and prolactin in *Andrias davidianus*: cDNA cloning, tissue distribution and phylogenetic analysis. Gen. Comp. Endocrinol. 165, 177–180.

Yaparla, A., Wendel, E.S., Grayfer, L., 2016. The unique myelopoiesis strategy of the amphibian *Xenopus laevis*. Dev. Comp. Immunol. 63, 136–143.

Zhang, P., Chen, Y.Q., Liu, Y.F., Zhou, H., Qu, L.H., 2003. The complete mitochondrial genome of the Chinese giant salamander, *Andrias davidianus* (Amphibia: Caudata). Gene 311, 93–98.

Zhang, Q.Y., Gui, J.F., 2015. Virus genomes and virus-host interactions in aquaculture animals. Sci. China Life Sci. 58, 156–169.

Zhu, R., Chen, Z., Wang, J., Yuan, J., Liao, X., Gui, J., Zhang, Q., 2014a. Extensive diversification of MHC in Chinese giant salamanders *Andrias davidianus* (Anda-MHC) reveals novel splice variants. Dev. Comp. Immunol. 42, 311–322.

Zhu, R., Chen, Z., Wang, J., Yuan, J., Liao, X., Gui, J., Zhang, Q., 2014b. Thymus cDNA library survey uncovers novel features of immune molecules in Chinese giant salamander *Andrias davidianus*. Dev. Comp. Immunol. 46, 413–422.